Am J Transl Res 2026;18(5):4387-4397
www.ajtr.org /ISSN:1943-8141/AJTR0171852

Original Article

Sodium hyaluronate/lysine nanoparticles loaded with si-VEGF-A inhibits corneal neovascularization

Dan Li[1,2], Huiming Hua[1,3]

[1]School of Traditional Chinese Materia Medica, Shenyang Pharmaceutical University, Shenyang, Liaoning, China; [2]Shenyang Xingqi Pharmaceutical Co., Ltd., Shenyang, Liaoning, China; [3]Key Laboratory of Structure-Based Drug Design and Discovery, Ministry of Education, Shenyang Pharmaceutical University, Shenyang, Liaoning, China

Received February 3, 2026; Accepted May 15, 2026; Epub May 15, 2026; Published May 30, 2026

Abstract: Objective: This study designed sodium hyaluronate/lysine (SH/Lys)-based nanoparticles loaded with vascular endothelial growth factor A (VEGF-A) siRNA (V-SH/Lys), aiming to effectively treat corneal neovascularization (CNV) by specifically inhibiting the expression of VEGF-A. Methods: The particle size, zeta potential and stability of the V-SH/Lys nanoparticles loaded with si-VEGF-A were tested. The effects of V-SH/Lys nanoparticles on the tube formation and migration of vascular endothelial cells were evaluated through Transwell, cell scratch assay and cell tube formation assay. A rat model of CNV was established, and the extent of the neovascularization was quantified. The levels of tumor necrosis factor-alpha (TNF-α) and interleukin-6 (IL-6) in the cornea were also measured. The safety of V-SH/Lys nanoparticles was evaluated through cytotoxicity tests on corneal epithelial cells and pathological examinations of rat fundus tissues. Results: The V-SH/Lys nanoparticles exhibited a particle size of 204.5 ± 38.3 nm, a zeta potential of +17.90 ± 6.46 mV, and demonstrated good stability as shown by high performance liquid chromatography (HPLC). In vitro experiments demonstrated that V-SH/Lys could block formation of the tubular structures and migration of vascular endothelial cells. In the CNV model induced by corneal alkali burn in rats, the area of new blood vessels in the V-SH/Lys group was smaller than that in the control group ($P<0.01$), and the levels of corneal inflammatory factors (TNF-α, IL-6) were significantly reduced. Moreover, V-SH/Lys nanogel exhibited no obvious toxicity to corneal epithelial cells, and no abnormalities were observed in the rat fundus tissues, indicating its favorable safety profile. Conclusion: This study has confirmed that V-SH/Lys nanoparticles, by targeting and regulating VEGF-A, provide an efficient, safe and non-invasive treatment strategy for CNV, and have potential for clinical application.

Keywords: Sodium hyaluronate, lysine nanogel, si-VEGF-A, corneal neovascularization

Introduction

Corneal neovascularization (CNV) is a blinding ocular disease that is characterized by an increase in angiogenic factors in the cornea and the vessels at the limbus invade the cornea, which can damage the transparency of the cornea [1]. The etiology of CNV is complex and is typically associated with infections, traumatic diseases, immune diseases, and corneal transplantation [2]. Currently, the primary approaches for managing CNV include pharmacological interventions, non-pharmacological therapies, and surgical procedures [3]. However, these treatment methods present certain limitations such as poor long-term therapeutic effects, significant side effects, and high recurrence rates [4]. Therefore, there is an urgent need to research a therapeutic agent free of adverse effects for the effective treatment of CNV.

The formation of corneal neovascularization is caused by the disruption of the balance between angiogenic factors and anti-angiogenic factors. Various pro-angiogenic factors, including vascular endothelial growth factor (VEGF), angiopoietin, endothelial secreted protein, platelet-derived growth factor, and pericytes, all participate in one or more stages of the angiogenic switch [5]. In recent years, extensive research has focused on therapeutic approaches directed at vascular endothelial cells to address CNV. The VEGF family consists

https://doi.org/10.62347/QHNA2139

of multiple members. Among them, VEGFA plays a central role in regulating the migration, proliferation and microvascular formation of vascular endothelial cells. VEGFA is a critical regulator of angiogenesis. Its aberrant overexpression in ocular tissues promotes the formation of new blood vessels, thereby leading to the pathogenesis of various ocular diseases [6]. Clinically, numerous commercialized antibody-based drugs are available for intravitreal injection. These agents bind to VEGF-A and prevent its interaction with VEGFRs. By doing so, they inhibit the generation of neovessels controlled by this signaling pathway and exert therapeutic effects on retinal and choroidal tissues associated with neovascularization [7]. The ability of siRNA to efficiently degrade target mRNA has garnered extensive attention in recent years. However, the cellular uptake of siRNA is hindered by the electrostatic repulsion between the negatively charged cell membrane and the exposed, negatively charged siRNA. Studies have shown that positively charged liposomes can efficiently encapsulate DNA and transfer it into cells [8]. It is worth noting that nanotechnology has also made significant breakthroughs in the treatment of CNV [9]. Zhang's team developed CPI nano particles, which can effectively inhibit the migration of vascular endothelial cells and the formation of new blood vessels [10]. Liu's team reported NCCR (derived from neutrophil-engineered nanovesicles as therapeutic drugs), which is a multi-dimensional CNV treatment method combining anti-VEGF therapy and photodynamic therapy [11]. In the past decade, nanotechnology has made significant progress in CNV research [12]. Sodium hyaluronate is an endogenous substance found in the eye, and compared to synthetic polymers, it better mimics the corneal microenvironment and reduces foreign body irritation. To further enhance therapeutic efficacy and address the limitations of traditional carriers, such as poor permeability and uncertain biosafety, this study employed a novel sodium hyaluronate/lysine (SH/Lys) nanocarrier.

In this study, the siRNA sequence of VEGF-A was chemically modified, and a SH/Lys nanomedicine loaded with siVEGF-A was prepared. Through in vitro and in vivo experiments, the inhibitory effect of this drug on corneal neovascularization was found to be good. Besides that, the animal safety assessment results indicated that the drug has good safety.

Materials and methods

siRNA

The cells were inoculated into 6-well plates and transfected when they grew to approximately 70%. To enhance the efficacy of the siRNA and reduce its potential toxicity, si-VEGF-A (Sense: 5'-CAACAAAUGUGAAUGCAGACC-3'; Antisense: 3'-UCUGCAUUCACAUUUGUUGUG-5') was chemically modified with 2'-Ome [13] and 2'-F [14] substitutions. The modified si-VEGF-A was transfected into the cells using Lipofectamine 3000 and incubated under standard conditions in a cell culture incubator. After transfection, the medium was replaced with complete growth medium for continued culture.

Preparation of V-SH/Lys nanogel

Ten mg of sodium hyaluronate (Shandong Zhongshan Biotechnology Co., Ltd., Rizhao, China) was dissolved in 10 mL PBS buffer (pH 7.4). Then 190 mg of 1-ethyl-3-(3-dimethylamino propyl) carbodiimide hydrochloride (EDC) was added and the mixture was stirred at room temperature in the dark for 30 minutes. Subsequently, 1 mg lysine (Guangzhou Anxin Pharmaceutical Co., Ltd., Guangzhou, China) was dissolved in 10 mL phosphate buffered saline (PBS) buffer, added drop by drop, and stirred for 30 minutes. After the reaction at 4°C for 16 hours, the mixture was placed in a dialysis bag (MWCO: 10 kDa) and dialyzed for 48 hours to obtain SH/Lys hydrogel. Ten mL of SH/Lys hydrogel was mixed with 1 mL of aqueous solution containing 1 mg of targeted peptide-siRNA conjugate at 4°C and gently stirred by magnetic stirring overnight to complete drug loading. The obtained nanocomplex suspension was diluted to a siRNA concentration of 20 μM. Benzalkonium chloride was added, and the pH was adjusted to 7.2-7.4 using NaOH, and the osmotic pressure was adjusted to 280-320 mOsm/L using sodium chloride. Finally, the solution was filtered sterilized using a 0.22 μm sterile filter and aliquoted into sterile eye drop vials, thus obtaining the final eye drop formulation.

Stability testing

The stability was tested using high-performance liquid chromatography. A Sepax Zenix SEC-100 (7.8 × 300 mm, 3 μm, 100 A) chromatographic column was employed, and the detection was carried out using a mobile phase of 150 mM phosphate solution (pH 7.0) + 100 mM NaCl.

Cell culture

HUVEC cells were purchased from Wanwu Biological Company (Hefei, China). The cells were seeded in Dulbecco's modified eagle medium (DMEM) medium with 10% fetal bovine serum (FBS). After the cells adhered and reached confluence, they were trypsinized and passaged. Third-passage cells in the logarithmic growth phase were used for subsequent experiments.

Alkali burn model in SD rats

SPF-level SD rats (male, 8 weeks old, weighing 180-220 g each) were purchased from Changsheng Biotechnology Company (Benxi, China). Prior to the experiment, all animals were screened using a slit lamp to ensure the absence of ocular abnormalities. A corneal alkali burn model was established in the rats as follows: anesthesia was induced by intraperitoneal injection of 20 mg/mL sodium pentobarbital, followed by topical ocular anesthesia with oxybuprocaine hydrochloride eye drops administered three times. A circular filter paper disc (3 mm in diameter) soaked in alkali solution (1 mol/L NaOH) was applied to the central cornea of the right eye for 40 seconds, after which the conjunctival sac was rinsed with normal saline for 2 minutes. Successful model induction was confirmed by the appearance of a grayish-white opacity in the central cornea and blurred iris texture. Rats with successfully induced corneal injury were randomly assigned into four groups (n = 6 per group): Model group, SH/Lys group, siRNA group, and V-SH/Lys group. Each group was administered eye drops to the eye surface, three times a day, for a total of 14 days. The behavioral changes of the rats after eye drops were observed daily, including whether they shook their heads, scratched their eyes, or blinked. This experiment was reviewed by the animal experiment Ethics Committee of Shenyang Xingqi Pharmaceutical Co., Ltd. (IACUC-20251205-0254), and the experimental process strictly adhered to the requirements for animal welfare.

Evaluation of corneal neovascularization in the alkali burn model

After pupil dilation, corneal images of the right eye in the SD rat alkali-burn model were captured under 20× magnification using a stereomicroscope to assess neovascularization. The area of corneal neovascularization was calculated using the following formula: $S = C/4 \times 3.14 \times [r^2 - (r - l)^2]$. In this equation, S represents the neovascularized area, C represents the clock hours involved, r represents the corneal radius, and l represents the length of invasion from the limbus into the cornea.

Enzyme-linked immunosorbent assay (ELISA) assay

Fourteen days later, the rats in each group were euthanized using the CO_2 method. The corneal tissues were extracted, washed with normal saline, and then ground and homogenized. The homogenates were centrifuged at 5,000 rpm for 10 min, and the supernatants were collected. According to the operation steps provided in the ELISA kit manual, the expression levels of inflammatory factors were detected using a microplate reader.

Cell counting kit-8 (CCK-8) assay

The HUVEC cells were inoculated into 96-well plates and cultured overnight in a 37°C, 5% CO_2 incubator. Then, different concentrations of V-SH/Lys were added and the culture was continued for 24 hours. Ten μL of CCK-8 solution was added to each well and the incubation was continued for another 4 hours. The absorbance values of each well were measured using an enzyme detector at 450 nm.

Live/dead cell assay

Cells were detached using 0.5% trypsin, collected by centrifugation, and resuspended in serum-free buffer. Next 200 μL cell suspension was mixed with 100 μL of Calcein AM/propidium iodide staining solution and incubated in the dark for 15-20 minutes. Cells were then observed under a fluorescence microscope.

Cell migration assay

Serum-free medium was placed in the upper chamber of the Transwell chamber, and medium with 10% FBS was added to the lower chamber. Cell suspension was added to the upper chamber (200 μL per well) and incubated in a 37°C incubator. After incubation, the cells were stained with crystal violet. Cells were removed that did not migrated in the upper chamber, and cells that migrated into the lower chamber were counted.

Wound healing assay

The cells were inoculated into 6-well plates (5-10 × 10^5 cells per well), and further cultured until the cells covered the entire plate. A scratch was made on the cell surface using a 20 μL pipette. The cell debris was washed off with PBS, and fresh serum-free medium was added. The plates were placed in a 37°C, 5% CO_2 incubator. Images of the cells were taken at 0 h and 24 h, and the area of cell migration was quantified using ImageJ.

Tube formation assay

The HUVEC cells were digested with trypsin, centrifuged for sedimentation, and then resuspended. The frozen-thawed Matrigel matrix gel was spread on a 96-well plate, bubbles were removed, and then placed in a 37°C incubator for solidification. A cell suspension (approximately 20,000 cells per well) was added to each well, and the plate was placed back in the incubator for 8 hours of incubation. The tubular structures were photographed under an inverted microscope, and the number of formed tubular structures was quantified using ImageJ.

Statistical analysis

All data are expressed as mean ± standard deviation and were statistically evaluated using GraphPad Prism 8.0. Group comparisons were performed using t-tests and one-way ANOVA followed by Tukey's test to assess significant differences. For multiple groups with time variables, repeated measures ANOVA was employed. Statistical significance was defined as a *P* value less than 0.05.

Results

Preparation of V-SH/Lys nanoparticles

Agarose gel electrophoresis results showed that when SH/Lys concentration reached 1 mg/mL, the siRNA band was almost undetectable, indicating that siRNA had been completely encapsulated. Therefore, 1 mg/mL was used for the synthesis of SH/Lys (**Figure 1A**). The average particle size of SH/Lys was approximately 198.5 ± 36.7 nm. After loading si-VEGF-A, the particle size of V-SH/Lys slightly increased to 204.5 ± 38.3 nm, indicating that incorporating si-VEGF-A into the pores of SH/Lys nanoparticles does not significantly alter its particle size (**Figure 1B**, **1C**). The potential of SH/Lys was approximately 90.32 ± 9.42 mV. The potential after loading si-VEGF-A was 17.90 ± 6.46 mV (**Figure 1D**).

Stability and quality of V-SH/Lys nanoparticles

The zeta potential and particle size of the V-SH/Lys nanoparticles were monitored for two weeks. There were no obvious changes in pure water at room temperature (**Figure 2A**, **2B**). The pH test results showed no significant differences in pH value at each time point (**Figure 2C**). Samples were taken at 0, 1, 2, 3 and 6 months for stability testing. The HPLC experiment showed that compared with the data at month 0, the peak height and area of the main peak remained basically the same in each time period, with RSD<0.5% (**Figure 2D**). Furthermore, the long-term stability test also demonstrated that the main peak had extremely high chemical stability (**Figure 2E**). The above results clearly indicate that V-SH/Lys nanoparticles have excellent long-term stability.

Safety of V-SH/Lys nanoparticles

Prior to the animal evaluation, we conducted experiments related to the biocompatibility of V-SH/Lys nanoparticles in HUVECs cells. The CCK8 results indicated that SH/Lys exhibited no significant cytotoxicity against HUVECs at concentrations ranging from 0.2 to 1 mg/mL, with cell viability remaining close to 100% (**Figure 3A**). Subsequently, a cell viability assay was performed using 1 mg/mL SH/Lys, and no obvious cell death was observed (**Figure 3B**).

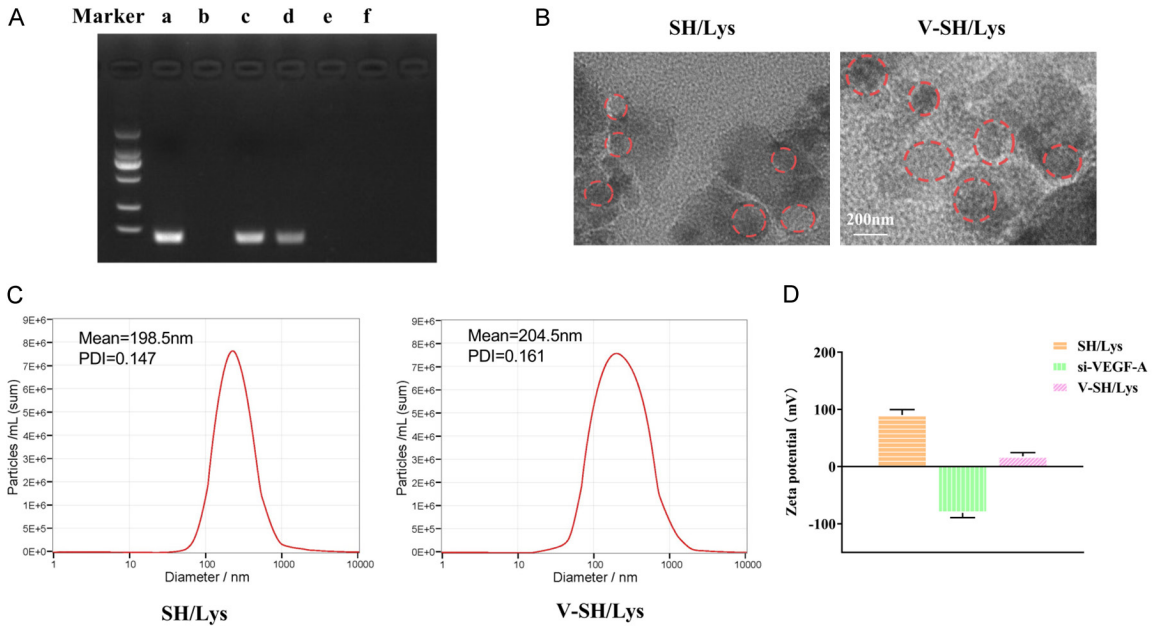

Figure 1. Preparation of V-SH/Lys nanoparticles. A. Gel electrophoresis analysis of si-VEGF-A. Unencapsulated si-VEGF-A (lane a), SH/Lys nanoparticles (lane b), 0.2 mg/mL SH/Lys loaded with si-VEGF-A (lane c), 0.5 mg/mL SH/Lys loaded with si-VEGF-A (lane d), 1 mg/mL SH/Lys loaded with si-VEGF-A (lane e), 2 mg/mL SH/Lys loaded with si-VEGF-A (lane f). B. TEM image of V-SH/Lys nanoparticles (200 μm, 80,000×). C. Size analysis of V-SH/Lys nanoparticles. D. The Zeta potential of V-SH/Lys nanoparticles. VEGF-A, vascular endothelial growth factor A; SH/Lys, sodium hyaluronate/lysine; TEM, transmission electron microscope.

The CNV rat model was established using the conventional method. Slit lamp photography showed that at 3 hours and 3 days with 1 mg/mL SH/Lys, there were no signs of eye redness, irritation or inflammation (**Figure 3C**). This indicates the safety of the V-SH/Lys in ocular applications, especially for the anterior structures of the eye, and is therefore reliable. Therefore, 1 mg/mL SH/Lys was used for further CNV model studies.

In vitro study of V-SH/Lys nanoparticles

Next, we investigated the effects of 1 mg/mL V-SH/Lys nanoparticles on the migration and tube formation abilities of HUVEC cells. The Transwell assay and wound healing assay verified that V-SH/Lys prominently inhibited the migration of HUVEC cells (**Figure 4A**, **4B**). Furthermore, V-SH/Lys nanoparticles also significantly hindered the tube formation of HUVEC cells (**Figure 4C**).

V-SH/Lys nanoparticles inhibits corneal neovascularization in rats

In the first two days after the alkali burn, new blood vessels began to form at the edge of the cornea and gradually extended towards the center of the cornea. On the 3rd, 7th, and 14th days, the severity of CNV in each group was evaluated. No significant difference was observed between the model group and the SH/Lys group. Compared with si-VEGF-A group, the V-SH/Lys group exhibited significantly reduced vascular length and area (**Figure 5A**). Fourteen days later, the levels of inflammatory factors in the corneal tissues of CNV rats were detected. The ELISA results showed that the levels of TNF-α and IL-6 in V-SH/Lys group of rats were clearly lower than those in the si-VEGF-A group (**Figure 5B**, **5C**).

Discussion

CNV is a severe ocular surface disorder typically caused by keratitis, corneal transplantation, or ocular trauma. In severe cases, it can lead to vision loss or even blindness. Currently, the clinical treatments for CNV mainly include pharmacological interventions and surgical procedures. Pharmacological treatments commonly include glucocorticoids, non-steroidal anti-inflammatory drugs (NSAIDs), and cyclosporine A; surgical options include argon laser

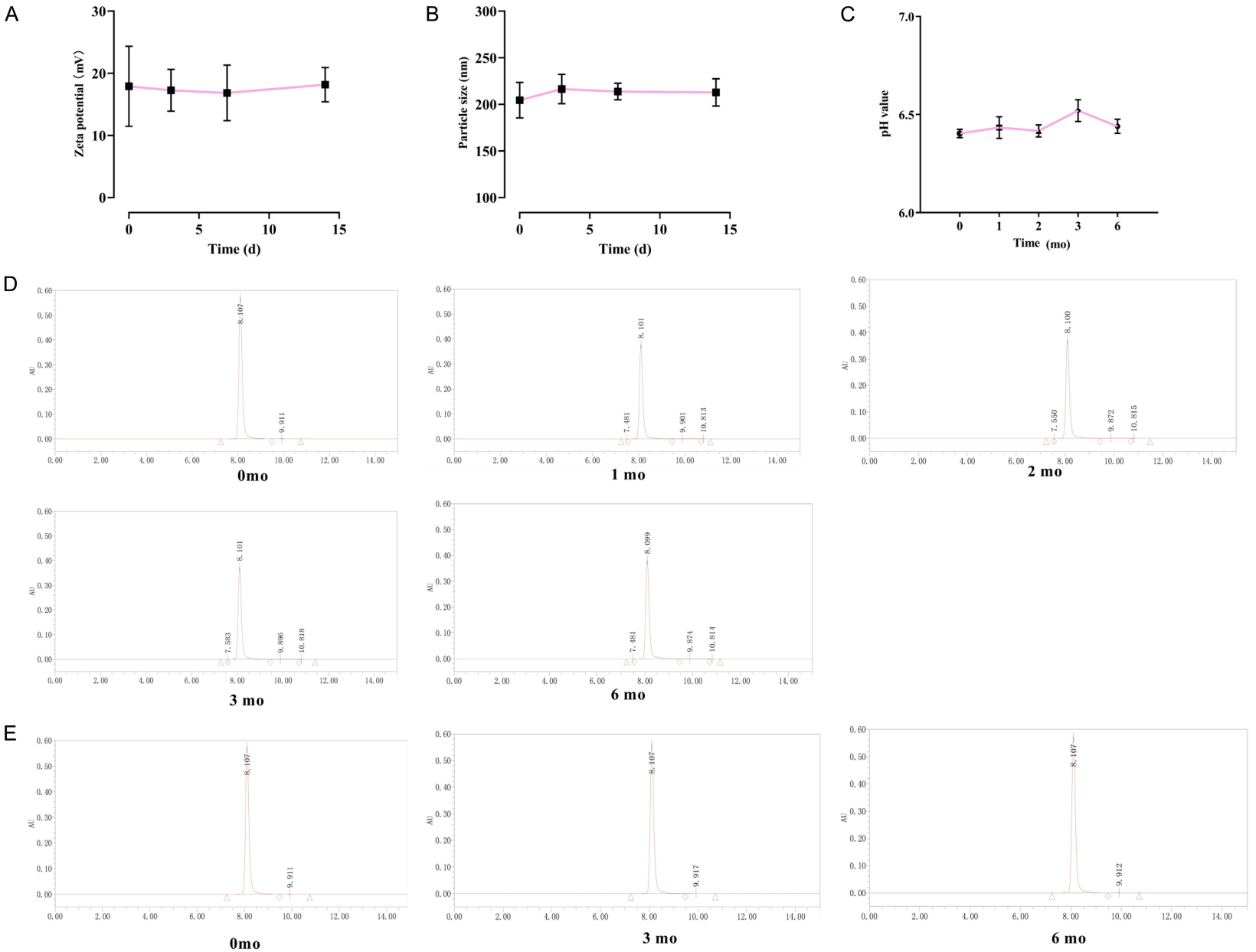
A
Zeta potential (mV)
Time (d)
B
Particle size (nm)
Time (d)
C
pH value
Time (mo)
D
0mo
1 mo
2 mo
3 mo
6 mo
E
0mo
3 mo
6 mo

Figure 2. Stability and quality of V-SH/Lys nanoparticles. A. The zeta potential changes of V-SH/Lys nanoparticles. B. The particle size variation of V-SH/Lys nanoparticles. C. The pH value changes of V-SH/Lys nanoparticles. D, E. HPLC was used to detect the stability of V-SH/Lys nanoparticles at different time points. HPLC, high performance liquid chromatography.

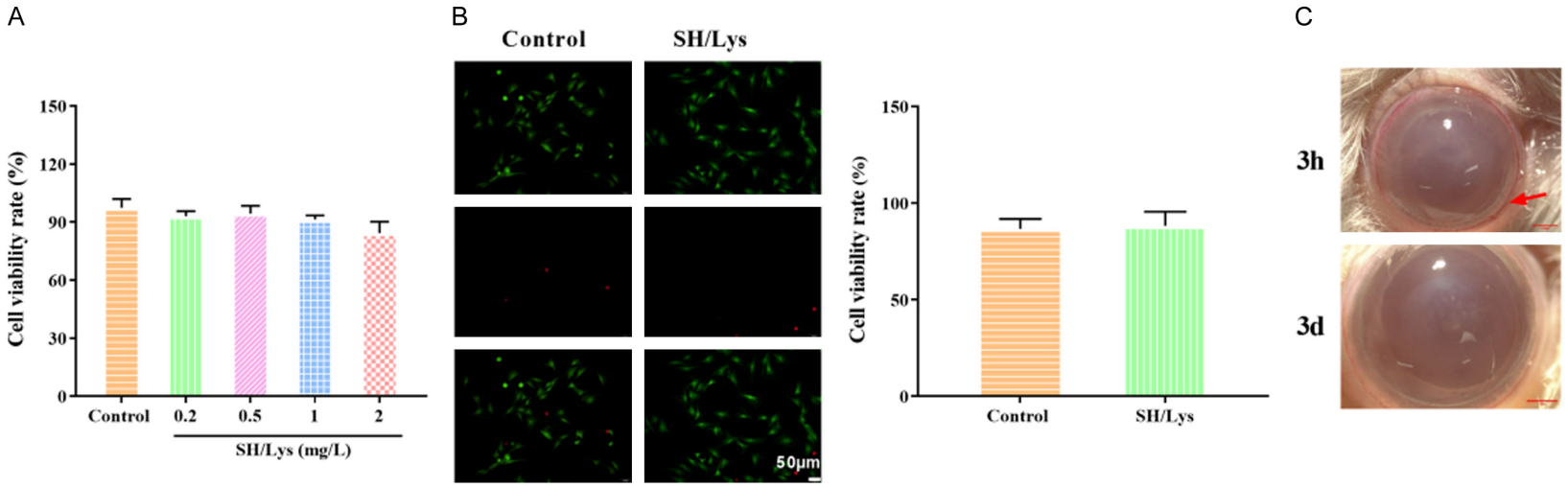

Figure 3. Safety of V-SH/Lys. A. The CCK-8 assay was used to investigate the effects of different concentrations of SH/Lys on the cell viability of HUVECs. B. The live/dead cell assay was conducted to examine the role of SH/Lys on cell death (50 μm, 200×). C. Slit-lamp examination of the CNV rat model. CCK-8, cell counting kit-8; CNV, corneal neovascularization.

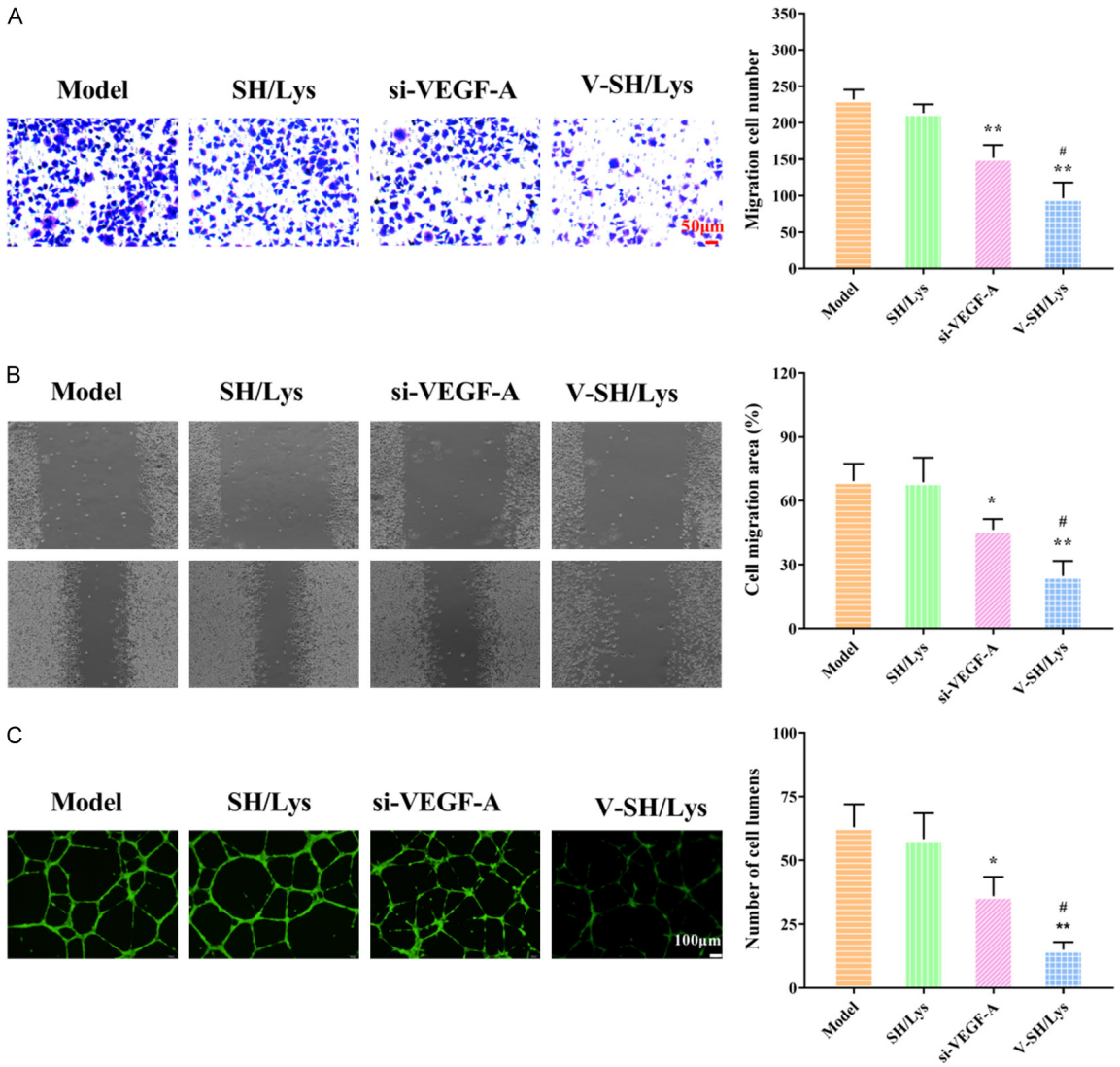

Figure 4. In vitro study of V-SH/Lys nanoparticles. A. The Transwell assay was employed to evaluate the impact of V-SH/Lys nanoparticles on the migratory capacity of HUVEC cells (50 μm, 200×). B. Wound healing assay was employed to evaluate the impact of V-SH/Lys nanoparticles on the migratory capacity of HUVEC cells. C. Cell tube formation assay was utilized to measure the effect of V-SH/Lys nanoparticles on the tube formation ability of HUVEC cells (100 μm, 100×). *P<0.05, **P<0.01, compared to the Model group; #P<0.05, compared to the si-VEGF-A group.

therapy and photodynamic therapy [15]. However, these therapeutic strategies are still limited by several drawbacks, such as low drug bioavailability, significant side effects, and the need for frequent administration. Meanwhile, single-target treatment strategies are prone to drug resistance, and the therapeutic effect is often not satisfactory, especially in patients with severe CNV, where conventional therapies are difficult to achieve satisfactory treatment results. With the continuous advancement of bio-nanotechnology, nanotechnology has provided revolutionary strategies for the treatment of CNV [16]. The bioavailability of traditional drugs is only 1%-5%, because the barrier of the ocular surface structure prevents the penetration of drugs [12]. This study developed a sodium hyaluronate/lysine nanoparticle drug loaded with si-VEGF-A, and investigated its mechanism on corneal neovascularization in rats.

Our research has revealed that the V-SH/Lys nanoparticles can significantly inhibit the migration and tube formation abilities of HUVEC

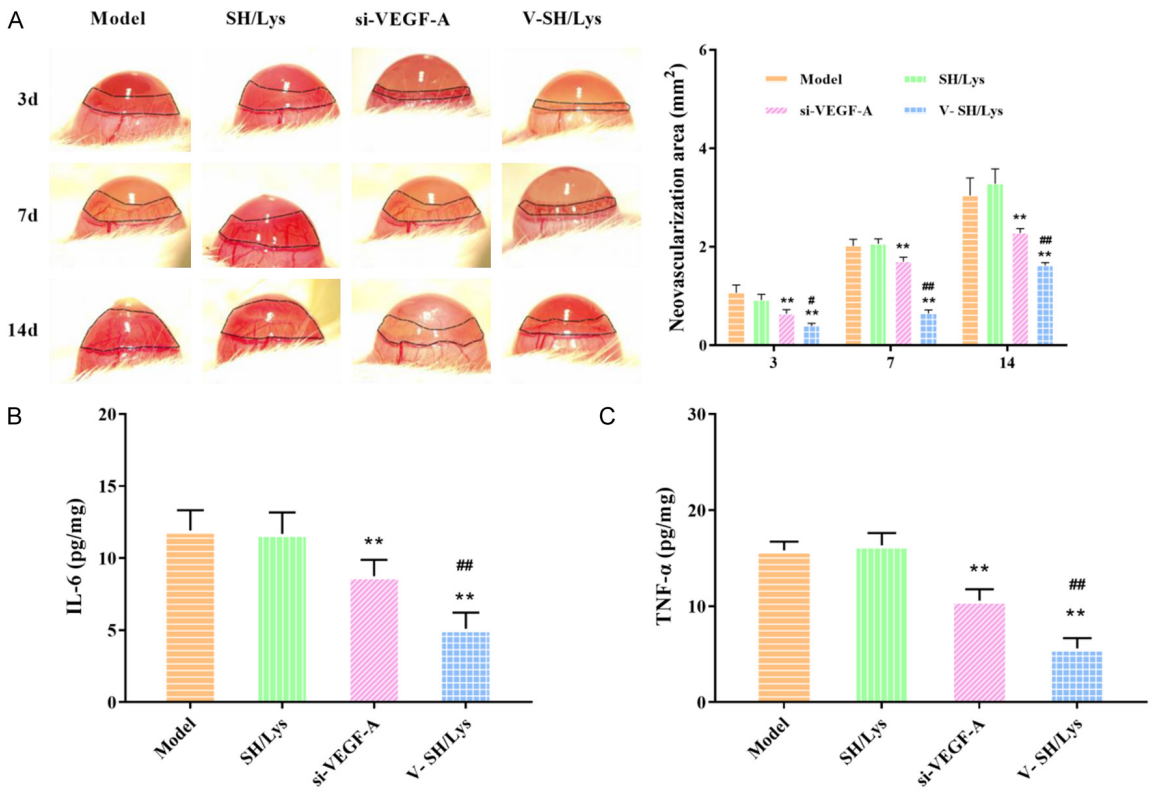

Figure 5. V-SH/Lys inhibits corneal neovascularization in rats. A. The vascular growth area of each group of CNV model rats. B. IL-6 content in corneal tissue. C. TNF-α content in corneal tissue. **P<0.01, compared to the Model group; #P<0.05, ##P<0.01, compared to the si-VEGF-A group. IL-6, interleukin-6; TNF-α, tumor necrosis factor-alpha.

cells. Furthermore, the nanoparticles effectively reduced the area of corneal neovascularization in a rat model. As a key factor driving angiogenesis within the VEGF family, VEGF-A is critically involved in the pathogenesis of CNV [17]. By binding to VEGFR, VEGF-A stimulates endothelial cell proliferation and migration, thereby leading to vascular leakage and the formation of new blood vessels [18]. A previous study has demonstrated that inhibiting VEGF significantly suppresses neovascularization in mouse models [19]. Anti-VEGF agents specifically bind to VEGFRs, thereby reducing vascular leakage and inhibiting the formation of new blood vessels. Common anti-VEGF drugs include ranibizumab, aflibercept, bevacizumab, and conbercept [20]. In the present work, the expression of VEGF-A was specifically downregulated using small interfering RNA technology.

Sodium Hyaluronate is the sodium salt of Hyaluronic Acid (HA), and it is widely used as an adjunctive ophthalmic drug in clinical practice [21, 22]. A study has shown that adding sodium hyaluronate to conventional anti-inflammatory treatment can significantly alleviate the dry eye symptoms of patients after cataract surgery [23]. Most importantly, sodium hyaluronate exerts anti-inflammatory effects by inhibiting bladder mucosal inflammation through blocking the activation of the IL-6/JAK2/Stat3 signaling pathway [24]. The administration of sodium hyaluronate significantly reduced the levels of IL-1 and IL-6 in patients with knee osteoarthritis, thereby promoting the recovery of joint function [25]. Our study also demonstrated that V-SH/Lys nanoparticles could reduce the levels of TNF-α and IL-6, exhibiting favorable anti-inflammatory properties. Furthermore, the V-SH/Lys nanoparticles possess excellent stability and safety. This is attributed to the high biocompatibility of sodium hyaluronate with the corneal stroma. Furthermore, the carboxyl groups on its molecular chain can form stable electrostatic interactions with lysine, thereby enhancing the stability of the nanoparticles [26]. This design enables the nanogels to remain stable in the

ocular surface environment while releasing siRNA in the acidic inflammatory microenvironment (such as neovascular areas). This strategy circumvents the rapid degradation associated with traditional protein drugs, thereby achieving effective ocular surface drug delivery.

The V-SH/Lys nanoparticles demonstrated good anti-CNV activity in animal models, suggesting its potential for application in the treatment of neovascular eye diseases. However, there are still some key issues that require further exploration. Since the corneas of rats are avascular, and the rat alkali burn model still has certain differences from the pathological process of human CNV (which may be caused by inflammation and infection), it is necessary to establish primate animal models in the future to more accurately assess the therapeutic effects. Moreover, although no obvious toxic reactions were observed in the short term, it is still necessary to monitor the long-term retention of the V-SH/Lys nanoparticles in the eye and the possible metabolic effects.

Conclusion

In conclusion, this study constructed a sodium hyaluronate/lysine nanoparticle drug loaded with si-VEGF-A, which significantly inhibits the formation of corneal neovascularization and exhibits favorable stability and safety. This provides a valuable reference for the development of treatment methods for CNV.

Disclosure of conflict of interest

None.

Address correspondence to: Dan Li, School of Traditional Chinese Materia Medica, Shenyang Pharmaceutical University, Shenyang Xingqi Pharmaceutical Co., Ltd., Shenyang, Liaoning, China. E-mail: 18240145238@163.com; Huiming Hua, School of Traditional Chinese Materia Medica, Key Laboratory of Structure-Based Drug Design and Discovery, Ministry of Education, Shenyang Pharmaceutical University, Shenyang, Liaoning, China. E-mail: huimhua@163.com

References

[1] Malyugin BE, Isabekov RS, Kalinnikova SY and Antonova OP. Methods of diagnosis and treatment of corneal neovascularization. Vestn Oftalmol 2023; 139: 86-92.

[2] Wen Y, Chen Z, McAlinden C, Zhou X and Huang J. Recent advances in corneal neovascularization imaging. Exp Eye Res 2024; 244: 109930.

[3] Drzyzga Ł, Śpiewak D, Dorecka M and Wyględowska-Promieńska D. Available therapeutic options for corneal neovascularization: a review. Int J Mol Sci 2024; 25: 5479.

[4] Feizi S, Azari AA and Safapour S. Therapeutic approaches for corneal neovascularization. Eye Vis (Lond) 2017; 4: 28.

[5] Mamikonyan V, Pivin E and Krakhmaleva D. Mechanisms of corneal neovascularization and modern options for its suppression. Vestn Oftalmol 2016; 132: 81-87.

[6] Wang H, Yang Y, Yu H, Ma L, Qi X, Qu J, Zhang X, Li N, Dou S, Liu X, Wei C and Gao H. Self-cascade APl nanozyme for synergistic anti-inflammatory, antioxidant, and ferroptosis modulation in the treatment of corneal neovascularization. Small 2024; 21: e2407751.

[7] Zeng Z, Li S, Ye X, Wang Y, Wang Q, Chen Z, Wang Z, Zhang J, Wang Q, Chen L, Zhang S, Zou Z, Lin M, Chen X, Zhao G, McAlinden C, Lei H, Zhou X and Huang J. Genome editing VEGFA prevents corneal neovascularization in vivo. Adv Sci (Weinh) 2024; 11: e2401710.

[8] Cao X, Wang C, Deng Z, Zhong Y and Chen H. Efficient ocular delivery of siRNA via pH-sensitive vehicles for corneal neovascularization inhibition. Int J Pharm X 2023; 5: 100183.

[9] Huang X, Wu Y, Li K, Xing W, Zhao N, Chen Z, Tao W, Zhou X, Yang M and Huang J. Advanced nanotechnology-driven innovations for corneal neovascularization therapy: smart drug delivery and enhanced treatment strategies. Adv Mater 2025; 37: e2508726.

[10] Zhang Y, Du Y, Zhou S, Liu Z, Li P and Du Z. Topical application of insulin encapsulated by chitosan-modified PLGA nanoparticles to alleviate alkali burn-induced corneal neovascularization. Nanoscale 2025; 17: 12323-12339.

[11] Liu X, Bi Y, Wei C, Zhang Y, Liu X, Guo X, Zhao L, Zhang J, Wang C and Gao H. Engineered neutrophil nanovesicles for inhibiting corneal neovascularization by synergistic anti-inflammatory, anti-VEGF, and chemoexcited photodynamic therapy. Adv Mater 2025; 37: e2411030.

[12] Huang XC, Xu GY, Yang PP, Wang L, Wang H and Hu Y. Recent progress on topical drug therapy for corneal neovascularization. ChemMedChem 2025; 20: e202500366.

[13] Robbins M, Judge A, Liang L, McClintock K, Yaworski E and MacLachlan I. 2'-O-methyl-modified RNAs act as TLR7 antagonists. Mol Ther 2007; 15: 1663-1669.

[14] Thirunavukarasu D, Chen T, Liu Z, Hongdilokkul N and Romesberg FE. Selection of 2'-Fluo-

ro-modified aptamers with optimized properties. J Am Chem Soc 2017; 139: 2892-2895.
[15] Gladkauskas T, Rundgren IM, Cristea I, Bukve T, Rødahl E and Bredrup C. Treatment options for alkali burn-induced corneal neovascularization: a comparative analysis of two tyrosine kinase inhibitors. Cornea 2025; 44: 1174-1181.
[16] Wei Y, Mai Y, Zhu R, Xu Y, Qi Q, Wen X, Zhao J, Zhang J, Guan J, Zhang X and Mao S. Intraocular fate of surface charge-dependent nanomicelles via topical administration: Posterior delivery and transport pathway. J Control Release 2025; 388: 114398.
[17] Xu C, Zhong W, Zhang H, Jiang J and Zhou H. Gap26 inhibited angiogenesis through the β-catenin-VE-cadherin-VEGFR2-Erk signaling pathway. Life Sci 2023; 328: 121836.
[18] Ribatti D. The discovery of the fundamental role of VEGF in the development of the vascular system. Mech Dev 2019; 160: 103579.
[19] Kuribayashi H, Iwagawa T, Kadohara S, Ohashi H, Kawaji C, Iida T, Suzuki T, Inokuchi Y, Soeda T, Saita K, Aihara M, Ebihara N, Miyai T and Watanabe S. Effects of dual inhibition of VEGF-A and Angpt-2 on angiogenesis and lymphangiogenesis in an Alkali-induced corneal injury model. Genes Cells 2025; 30: e70035.
[20] Chen Z, Zhang W, Mestanoglu M, Cursiefen C and Bock F. Promotion of vessel regression by local VEGF-A blockade improves the survival rate of corneal transplants. Exp Eye Res 2025; 261: 110652.
[21] Wang Y, Shi S, Zhang L, Wang S, Qin H, Wei Y, Wu X and Zhang M. Imatinib@glycymicelles entrapped in hydrogel: preparation, characterization, and therapeutic effect on corneal alkali burn in mice. Drug Deliv Transl Res 2024; 15: 171-184.
[22] Wen Y, Zhang X, Chen M and Han D. Sodium hyaluronate in the treatment of dry eye after cataract surgery: a meta-analysis. Ann Palliat Med 2020; 9: 927-939.
[23] Yusufoğlu E and Keser S. The effect of sodium hyaluronate on dry eye and corneal epithelial thickness following cataract surgery. Int Ophthalmol 2024; 44: 211.
[24] Ni Y, Zhao S, Yin X, Wang H, Guang Q, Hu G, Yang Y, Jiao S and Shi B. Intravesicular administration of sodium hyaluronate ameliorates the inflammation and cell proliferation of cystitis cystica et glandularis involving interleukin-6/JAK2/Stat3 signaling pathway. Sci Rep 2017; 7: 15892.
[25] Zhang F, Zhang J and Wang T. Meta-analysis of minimally invasive arthroscopy with sodium hyaluronate for wound healing of knee osteoarthritis treatment in the elderly. Int Wound J 2023; 21: e70474.
[26] Yoshizaki Y, Yamasaki M, Nagata T, Suzuki K, Yamada R, Kato T, Murase N, Kuzuya A, Asai A, Higuchi K, Kaji K, Yoshiji H and Ohya Y. Drug delivery with hyaluronic acid-coated polymeric micelles in liver fibrosis therapy. ACS Biomater Sci Eng 2023; 9: 3414-3424.